Hypertension Research (2017) 40, 552–561

www.nature.com/hr

ORIGINAL ARTICLE

MiR-126a-5p is involved in the hypoxia-induced endothelial-to-mesenchymal transition of neonatal pulmonary hypertension

Yan-ping Xu[1], Qi He[1], Zheng Shen[2], Xiao-li Shu[2], Chen-hong Wang[1], Jia-jun Zhu[3], Li-ping Shi[1] and Li-zhong Du[1]

Persistent pulmonary hypertension of the newborn (PPHN) is a clinical syndrome characterized by increased medial and adventitial thickness of the lung vasculature. The underlying mechanisms that regulate the cell phenotype alteration during PPHN remodeling are largely unknown. We randomly selected newborn rats that were exposed to hypoxia (10–12%) or room air for 2 weeks and used a microarray to identify the lung tissue microRNAs (miRNAs) involved in PPHN progression. The role of a key miRNA that affects the endothelial-to-mesenchymal transition (EndMT) in primary cultured rat pulmonary microvascular endothelial cells (RPMECs) was investigated. The expression of miR-126a-5p was elevated in the PPHN model according to microarray analysis. The relative expression of miR-126a-5p in RPMECs increased when they were exposed to hypoxia ($P<0.05$), consistent with the microarray results. Pecam1 expression decreased, whereas alpha-smooth muscle actin (α-SMA) increased in the hypoxic RPMECs. Knockdown of miR-126a-5p in RPMECs followed by treatment with hypoxia for 48 h resulted in a significant increase in the expression of Pecam1 and a reduction in α-SMA expression, with a simultaneous increase in PI3K (p85β) and phosphorylation of AKT at serine 473 compared with the negative control. Finally, the circulating miR-126a-5p concentration was upregulated in the PPHN model compared with healthy neonates. We concluded that hypoxia changed the cell homeostasis and that miR-126a-5p was upregulated in PPHN, which is partly responsible for hypoxia-induced EndMT. The mechanism underlying the upregulation of miR-126a-5p by hypoxia probably acts through the p85-β/p-AKT pathway.
Hypertension Research (2017) **40,** 552–561; doi:10.1038/hr.2017.2; published online 2 February 2017

Keywords: endothelial-to-mesenchymal transition; miR-126a-5p; persistent pulmonary hypertension of the newborn

INTRODUCTION

Despite marked improvements in medical care, ~1.9 in 1000 neonates are perinatally exposed to intermittent or chronic periods of hypoxia and are at risk for persistent pulmonary hypertension of the newborn (PPHN).[1] Compared with adults, the neonatal pulmonary vasculature is more susceptible to a hypoxic insult.[2–4] In the perinatal period, the pulmonary vasculature undergoes important maturational changes, and perturbation of this process by hypoxia may result in the failure of fetal circulation to initiate adaptive responses to support postnatal life, ultimately culminating in PPHN. PPHN contributes to neonatal hypoxemia, which is often refractory, and is associated with substantial morbidity and mortality.[5] The important features of the pulmonary vasculature in PPHN are typically the abnormal extension of smooth muscle into the peripheral arteries, together with pulmonary arterial wall thickening and muscularization[6–8] secondary to endothelial-to-mesenchymal transition (EndMT). EndMT is the process by which endothelial cells lose their cell-specific markers and morphology, and acquire a mesenchymal cell-like phenotype. EndMT is regulated by several complex signaling pathways.[9] However, the role of EndMT and the mechanisms regulating cell phenotype adaptation during PPHN remodeling are poorly understood.

microRNAs (miRNAs, miRs) are highly conserved noncoding RNA molecules that are 21–23 nucleotides in length and negatively regulate gene expression at the posttranscriptional level. They target numerous genes and thus potentially control signaling pathways.[10] Caruso *et al.*[11] were the first to report the dysregulation of miRNAs during the development of pulmonary arterial hypertension. They found that in two commonly used rodent models of pulmonary arterial hypertension (exposure to chronic hypoxia and monocrotaline insult in rats), miR-22, miR-30 and let-7f are downregulated, whereas miR-322 and miR-451 are upregulated.[11] Many miRNAs are dysregulated during disease, with consequences for cell-type-specific gene expression

[1]NICU, The Children's Hospital, Zhejiang University School of Medicine, Zhejiang Key Laboratory for Diagnosis and Therapy of Neonatal Diseases, Hangzhou, China; [2]Center Lab, Children's Hospital, Zhejiang University School of Medicine, Hangzhou, China and [3]Department of Neonatology, Women's Hospital, Zhejiang University School of Medicine, Hangzhou, China
Correspondence: Dr L-z Du, NICU, The Children's Hospital, Zhejiang University School of Medicine, Zhejiang Key Laboratory for Diagnosis and Therapy of Neonatal Diseases, 3333 Binsheng Road, Hangzhou 310051, China.
E-mail: dulizhong@zju.edu.cn
Received 15 September 2016; revised 27 November 2016; accepted 8 December 2016; published online 2 February 2017

disorders. Therefore, many miRNA-related therapeutic strategies have been developed to mitigate single miRNA-induced perturbations of gene expression in diseased tissues.

The mechanisms underlying hypoxia-induced neonatal pulmonary arterial remodeling and the associated EndMT remain unclear. Therefore, we used microarray to identify the miRNAs involved in the EndMT process. In addition, we focused specifically on molecules displaying expression changes during PPHN progression, and the role of a key miRNA that affects the signaling pathways involved in the phenotypic changes that occur during EndMT was investigated.

METHODS

Ethics statements

This study was approved by the Animal Experimental Committee of Zhejiang University. Animal care and all procedures were performed according to the Guidelines for the Care and Use of Laboratory Animals. The human study was approved by the local Institution Review Board and conducted according to the principles expressed in the Declaration of Helsinki. Written informed consent for participation in the study was obtained from the parents of infants.

Animals and lung tissue preparation

The investigation conformed to the Guide for the Care and Use of Laboratory Animals published by the US National Institutes of Health (NIH Publication No. 85-23, revised 1996). Sprague–Dawley rat pups were postnatally treated with chronic hypoxia to induce PPHN, as we have previously described.[12] We measured the body weight of the dams and pups, and intrauterine growth restriction pups were excluded. Briefly, rats were randomly divided into four groups ($n=10$ per group): (1) continuous hypoxia for 7 or 14 days, and (2) sham control in which rats were not subjected to hypoxia. Animals were anesthetized using sodium pentobarbital (50 mg kg^{-1}, i.p.), and the pups were killed immediately after hypoxia. Lung tissue was stored in liquid nitrogen for later RNA isolation, and protein extraction or fixed in formalin and embedded in paraffin for immunostaining. A flow chart of this process is shown in Figure 1.

Microarray analysis of miRNAs

Lung tissue was harvested from rats exposed to hypoxia for 14 days and control rats ($n=3$ per group). Mouse and Rat miRNA OneArray microarrays (MRmiOA v5, Phalanx Biotech Group, Palo Alto, CA, USA) were used, and all probes were printed in triplicate. Each slide was hybridized with samples containing 1 μg of RNA. The files were loaded into R version 2.12.1 (R Foundation, Vienna, Austria) for data analysis. The standard selection criteria to identify differentially expressed genes were established at log2 |Fold change| $\geqslant 0.585$ and $P<0.05$.

Quantification of miRNA and mRNA levels

Total RNA samples were extracted from lung tissues and rat pulmonary microvascular endothelial cells (RPMECs). The TaKaRa MiniBEST Universal RNA Extraction Kit, the miRNeasy Serum/Plasma kit (Qiagen, Hilden, Germany) and the qRT-PCR miRNA Detection Kit (Takara Biotechnology, Dalian, China) were used in conjunction with real-time PCR utilizing SYBR Green I for the quantification of miRNA transcripts. For quantification of platelet/endothelial cell adhesion molecule-1 (*Pecam1*), *Acta2*, S100 calcium-binding protein A4 (*S100a4*), and TGF-β2 transcripts, conventional real-time RT-PCR was carried out using the primers listed in Supplementary Table S1.

Immunohistochemistry and immunofluorescence staining

Four-micrometer paraffin-embedded lung sections were used for immunohistochemical analyses. The primary antibodies used were against alpha smooth muscle actin (αSMA) (1:100; Santa Cruz Biotechnology, Santa Cruz, CA, USA) and S100a4 (1:50; Abcam, Cambridge, UK). Neonatal RPMECs were isolated using a modification of a technique described previously.[13] Cells were exposed to 10% fetal bovine serum and endothelial cell growth factor (80 μg ml^{-1}) and were treated in the presence or absence of $CoCl_2$ (100 μmol l^{-1}, Sigma-Aldrich, St Louis, MO, USA) for 24, 48 or 72 h. The cells were characterized by routine fluorescence immunohistochemistry. The cells were incubated for 1 h with the mouse primary antibody anti-αSMA (1:50 dilution) and the rabbit primary antibody anti-S100a4 (1:50 dilution).

TGF-β2 ELISA

A TGF-β2 enzyme-linked immunosorbent assay (ELISA) (R&D Systems, Minneapolis, MN, USA, MB 200) was used to determine the total level of TGF-β2 in acid-activated cell culture supernatants as per the manufacturer's recommendations.

Western blot analysis

Whole-cell lysates or homogenized lung tissues that contained 20–50 μg of protein were subjected to 6, 8 or 15% SDS-polyacrylamide gel electrophoresis and transferred onto polyvinylidene fluoride membranes. The primary antibodies included those against PECAM1, αSMA, PI3 kinase p85β (p85β) (1:200, 1:600 and 1:200, respectively; from Santa Cruz Biotechnology), phospho-AKT (ser473) (p-AKT), AKT, PI3 Kinase p110 (p110α) (1:2000, 1:2000 and 1:1000, respectively; from Cell Signaling Technology, Beverly, MA, USA) and S100a4 (1:200; Abcam). The bands of the western blots were quantitated by densitometry and normalized to that of β-actin using Image-Pro Plus software (Media Cybernetics, Silver Spring, MD, USA). The data were converted to relative units normalized to β-actin (1:1000, Beyotime Institute of Biotechnology, Shanghai, China), which was designated as 1. To ensure the reproducibility of the results, each sample was assessed at least twice.

Oligonucleotides and transfection

miR-126 precursors, miR-126-5p inhibitors and negative control molecules were obtained from GeneChem (GeneChem, Shanghai, China) and transfected into RPMECs at a final concentration 10^7 TU ml^{-1}. The medium was changed after 8 h. The cells were cultured for 96 h and harvested for later analyses as described above.

Luciferase reporter assays

HEK293 cells were seeded at 1×10^5 cells per well in 24-well plates the day prior to transfection. For miR-126-5p target validation, the entire 3′UTR sequence of rat TGF-β2 was amplified by PCR and cloned into a T-vector (Promega, Madison, WI, USA). The mutant TGF-β2 3′UTR synthesized (GeneChem) was identical to the wild-type sequence, except for the seed region, where the complementary sequence was used. All transfections were carried out using Lipofectamine 2000 (Invitrogen, Carlsbad, CA, USA) according to the manufacturer's instructions. After 48 h of transfection, luciferase activities were measured using the Dual-Luciferase Reporter Assay System (Promega) and normalized to Renilla luciferase activity. All experiments were performed in duplicate with data pooled from three independent experiments.

Human study population

Neonates with clinical and echocardiographic signs of hypoxia-induced neonatal pulmonary hypertension (PH) who were admitted to the NICU at Children's Hospital, Zhejiang University School of Medicine, and healthy infants from the Neonatal Unit, Women's Hospital of Zhejiang University School of Medicine, from March 2014 to November 2014, were enrolled in the study following approval by the local Institution Review Board. Neonatal PH was defined as hypoxemia with echocardiographic findings of elevated pulmonary artery pressure, right-to-left shunting through a patent foramen ovale or patent ductus arteriosus, or both. Clinical signs were hypoxemia and a decrease in 'post-ductal' saturation as a result of right-to-left shunting. Echocardiography was routinely performed by an experienced pediatrician on suspicion of PH to confirm the diagnosis and to exclude congenital heart disease. The demographic data collected were gestational age at birth, birth weight, gender, 1-, 5-minute Apgar scores, mode of delivery and associated illness. Blood samples (1 ml) were obtained at admission at an age of 5 days. Blood was centrifuged at 3000 *g* for 10 min at room temperature immediately after collection to completely remove cell debris and then transferred to

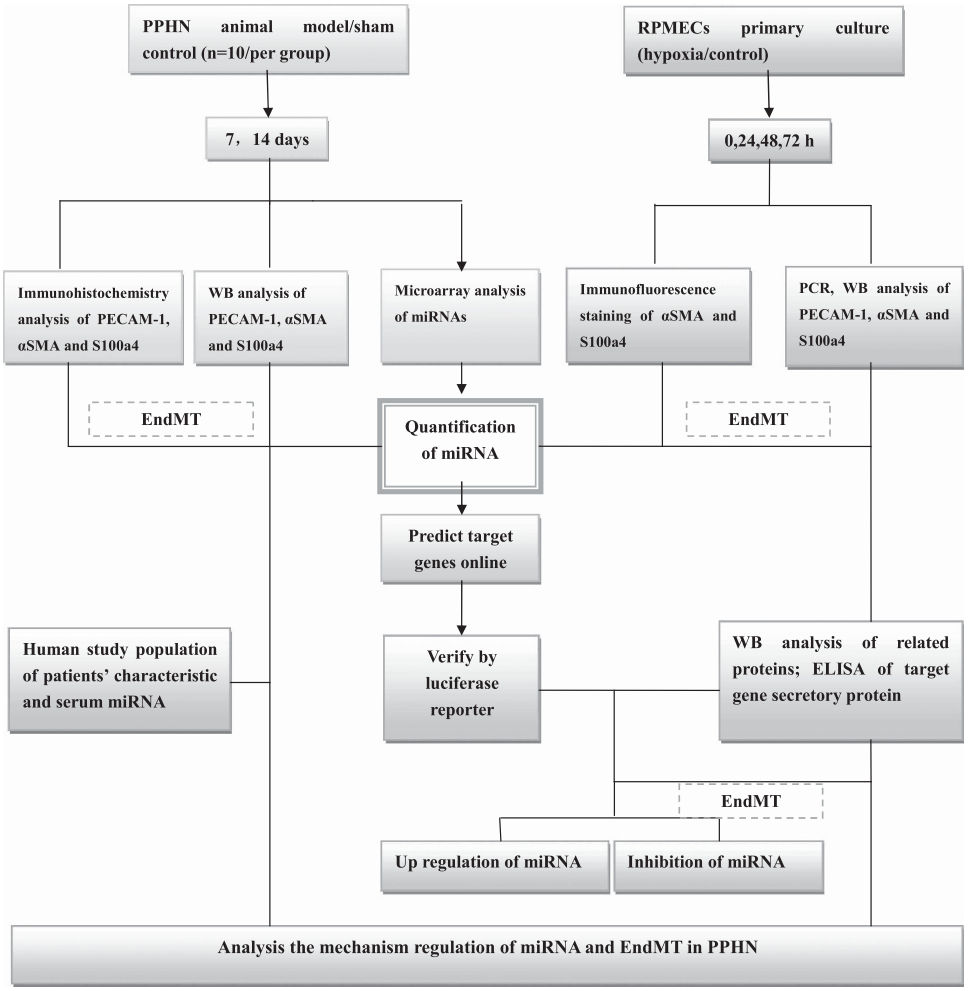

Figure 1 Flow chart. A full color version of this figure is available at *Hypertension Research* online.

RNase-/DNase-free tubes and stored at −80 °C until further processing. The miRNeasy Serum/Plasma Kit (Qiagen) and qRT-PCR miRNA Detection Kit (Takara Biotechnology) were used in conjunction with real-time PCR with SYBR Green I for quantification of miRNA transcripts with an ABI PRISM 7500 Sequence Detection System (Applied Biosystems, Foster City, CA, USA). Cycling conditions were 95 °C for 5 min, followed by 40 cycles of 95 °C for 15 s and 60 °C for 60 s. All PCR reactions were performed in triplicate, and U6 RNA was used as an internal control. The expression levels of miR-126a-5p were calculated relative to U6 miRNA using the equation $2^{-\Delta CT}$, where $\Delta CT = (CT^{miR\text{-}126\text{-}5p} - CT^{U6})$. In addition, blood gas analysis was performed concurrently. The oxygenation index and alveolar/arterial oxygen gradient (AaDO2), which are indicators of disease severity, were calculated. To assess the intensity of blood pressure support, a blood pressure support scoring system was used, depending on the intensity of the treatment necessary (score 0: no treatment; score 1: volume expansion and dopamine $\leqslant 5\ \mu g\ kg^{-1} min^{-1}$; score 2: dopamine >5 and $\leqslant 10\ \mu g\ kg^{-1}\ min^{-1}$; score 3: dopamine $>10\ \mu g\ kg^{-1}\ min^{-1}$ or dopamine+dobutamine $\leqslant 10\ \mu g\ kg^{-1}\ min^{-1}$; score 4: dopamine+dobutamine $>10\ \mu g\ kg^{-1}\ min^{-1}$; score 5: additional adrenaline and/or corticosteroids).[14,15]

Statistical analysis

The data are expressed as the mean ± s.e.m. or median (interquartile range) as appropriate. Statistical analysis was performed using Student's *t* test for two groups of data and using a 1-way ANOVA for multiple comparisons. Proportions were compared using X^2 analysis. Pearson's correlation coefficient was used to examine the association between the concentrations of serum miR-126a-5p with various oxygenation index, AaDO2 and blood pressure support scoring parameters. The *Z*-scores were used for clustering miRNAs using the commercial software for clustering microarray data. Values of $P<0.05$ were considered statistically significant. All data analyses were carried out using SPSS software for Windows (version 13.0; SPSS, Chicago, IL, USA).

RESULTS

Characterization of the miRNA profile in lung tissue of PPHN rats

To confirm whether small pulmonary arteries (lumen diameter (LD) $<100\ \mu m$) of neonatal rats with PH underwent EndMT, immunohistochemical staining for PECAM1, α-SMA and S100a4 was performed on paraffin-embedded lung tissue. Peripheral pulmonary arterioles were thickened, and muscularization was increased, as demonstrated by immunostaining for α-SMA and S100a4 (Figure 2). There were no significant differences found in the PECAM1 staining (Figure not shown). To identify miRNAs that may modulate the EndMT in PPHN, we first used miRNA arrays to survey miRNA expression levels in the lung tissue. Of the 1506 three repeat probes and 144 control probes, 363 miRNAs (~50.3% of the total 722 rat miRNAs) were detected. Six miRNAs had increased expression and two miRNAs had decreased concentrations in the PPHN model (Figure 3, Table 1). Because miR-19a-3p, miR-126a-5p, miR-218a-5p and let-7b-5p had not been reported in the pulmonary vascular system at the time we conducted this study, we decided to further analyze their roles in

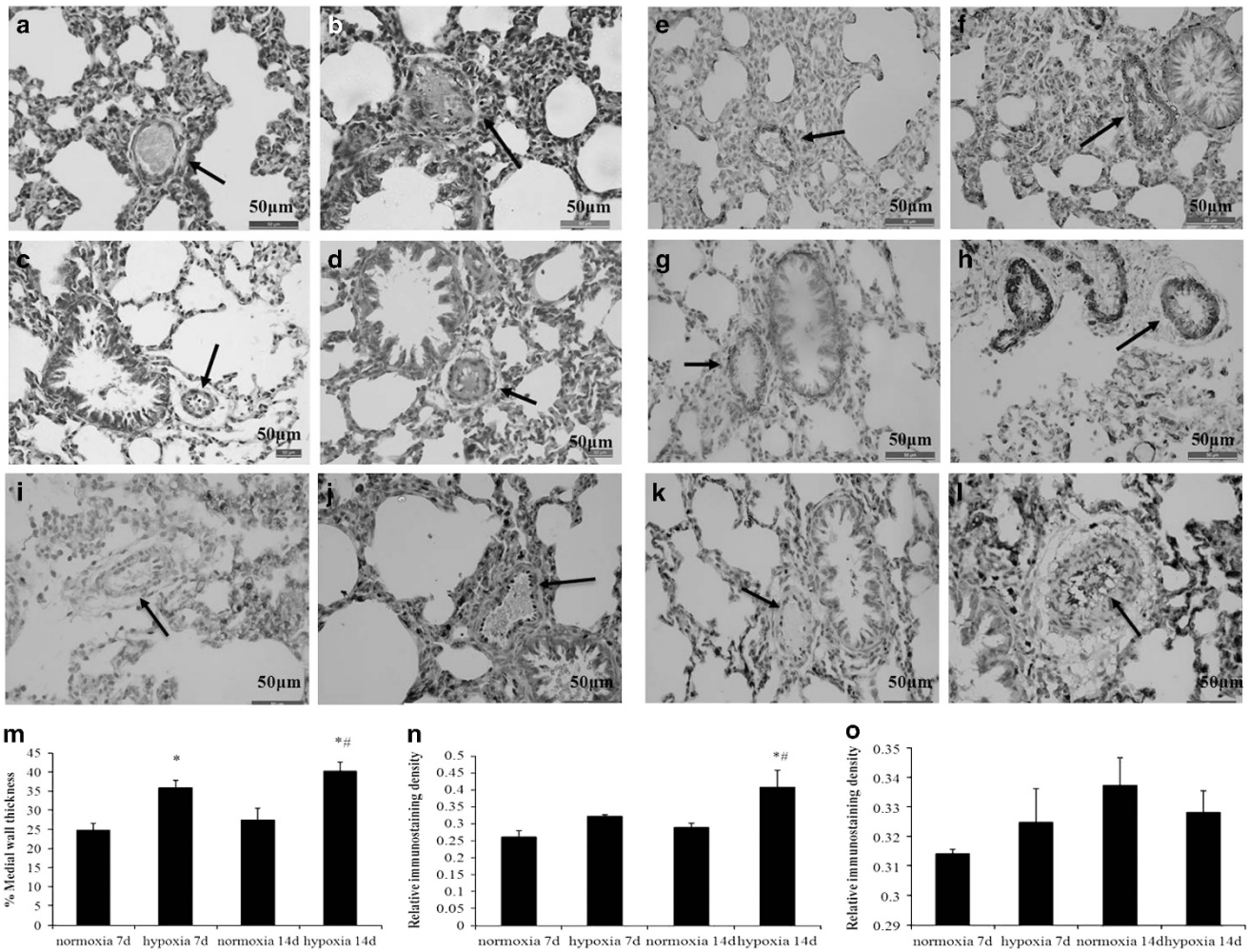

Figure 2 Photomicrographs of lung tissue sections from neonatal rats. (**a**) HE staining: normoxia for 7 days, (**b**) HE staining: hypoxia for 7 days, (**c**) HE staining: normoxia for 14 days and (**d**) HE staining: hypoxia for 14 days. (**e**–**h**) The α-smooth muscle actin staining (brown) in pulmonary vascular smooth muscle cells from small (lumen diameter (LD) <100 mm) vessels: (**e**) normoxia for 7 days, (**f**) hypoxia for 7 days, (**g**) normoxia for 14 days and (**h**) hypoxia for 14 days. (**i**–**l**) The S100a4 staining (brown) in pulmonary vascular endothelial cells from small (LD <100 mm) vessels: (**i**) normoxia for 7 days, (**j**) hypoxia for 7 days, (**k**) normoxia for 14 days and (**l**) hypoxia for 14 days. (**m**) The bar graphs represent the medial wall thickness percentage from pulmonary arteries. Medial wall thickness (%) $= 100 \times$ (medial wall thickness)/external diameter. (**n**, **o**) The relative immunostaining density for S100a4 in pulmonary arterial endothelium from samples treated with hypoxia for 14 days was significantly higher than that from the control ($P<0.05$). There was no statistically significant difference in the relative density of S100a4 from other cells between the PPHN group and the control. $^{*}P<0.05$ as compared with the normoxia group treated for 7 days; $^{\#}P<0.05$ as compared with the normoxia group treated for 14 days ($n=6$ per group). A full color version of this figure is available at *Hypertension Research* online.

the pulmonary vascular system. To confirm the expression of these four miRNAs, we applied real-time PCR and found out that the expression of miR-126a-5p was significantly higher and that of let-7b-5p was significantly lower in the PPHN model than in the control group ($P<0.05$; Figure 4a). The real-time PCR data of miR-126a-5p and let-7b-5p showed very similar results as the microarray, whereas there were no significant differences found for the other miRs (miR-19a-3 and miR-218a-5p).

Hypoxia-induced RPMECs underwent EndMT and expressed upregulated miR-126a-5p

As shown in Figures 5c and d, Supplementary Figures S1 and S2, after the treatment with hypoxia for 24–72 h, RPMECs underwent a morphological change from a cobblestone-like to a spindle-shaped appearance. RPMECs exposed to treatment with hypoxia or TGF-β2 appeared to be less confluent than the control. We treated cells with both hypoxia and TGF-β2, and most of the cells died. In addition, RPMECs showed decreased mRNA expression of the endothelial markers Pecam1 and increased mRNA expression of the mesenchymal markers α-SMA and S100a4 (Figure 5a). Meanwhile, TGF-β2 mRNA expression was simultaneously upregulated by the hypoxia treatment for 24–72 h compared with the normal control (Figure 5b). An increase in miR-126a-5p expression was observed when comparing normoxic cells to RPMECs subjected to hypoxia for 24–72 h, which is similar to the findings in the lung tissue of the PPHN animal model for miR-126a-5p (Figure 4b). Western blot analysis was used to assess the EndMT process in RPMECs induced by hypoxia. Hypoxia treatment markedly decreased the endothelial cell marker Pecam1 at 48–72 h and increased protein expression of the mesenchymal marker

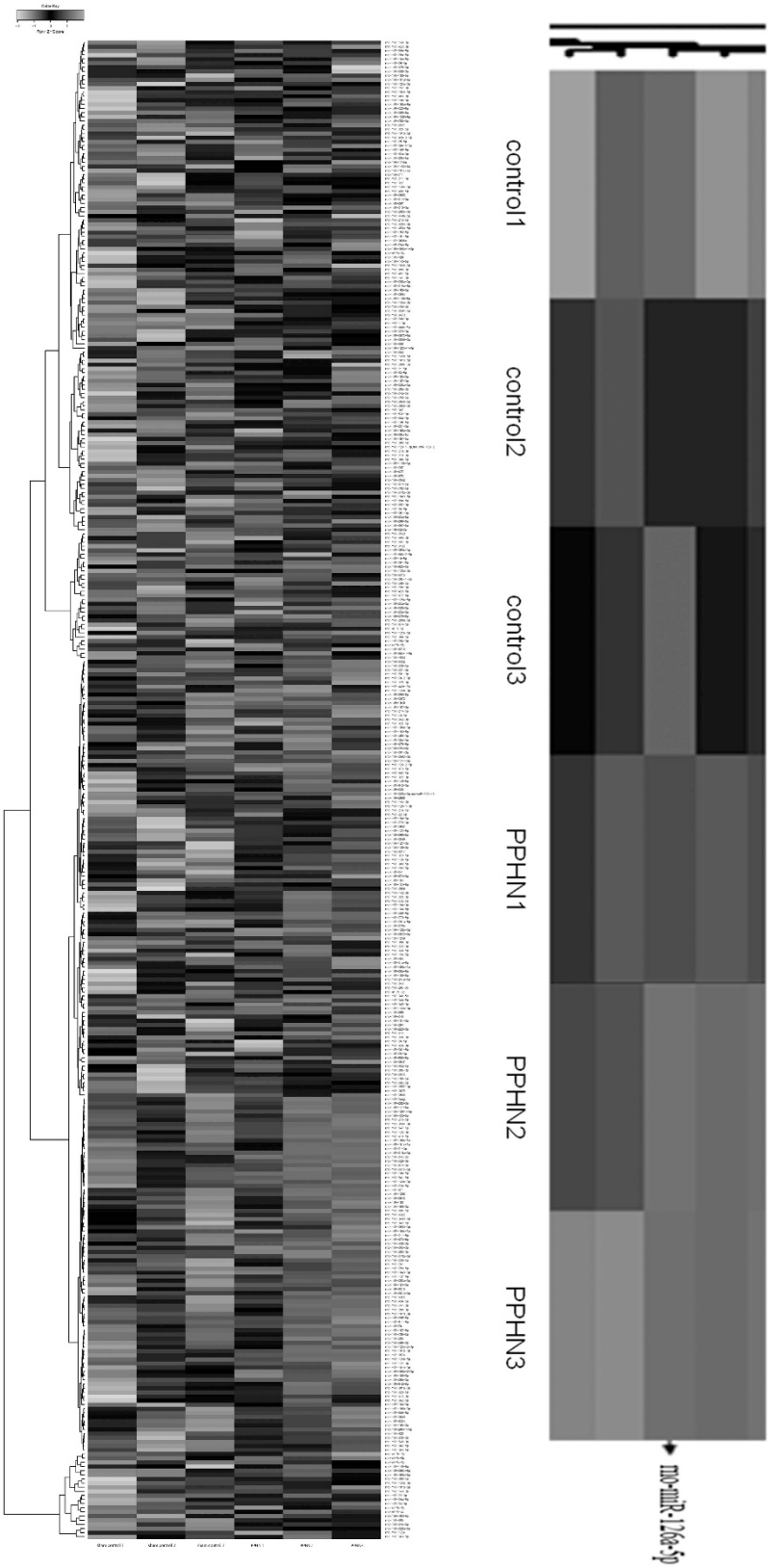

Figure 3 Cluster of 363 miRNA expression profiles from PPHN lung tissues (hypoxia 14 days) and sham control ($n=3$ per group). miRNA, microRNA; PPHN, persistent pulmonary hypertension of the newborn. A full color version of this figure is available at *Hypertension Research* online.

αSMA at the same time (Figure 5; EFG). However, S100a4 protein was almost not detected in the western blot analysis of RPMECs.

To explore the role of miR-126a-5p in the hypoxia-induced EndMT of RPMECs, RPMECs were transfected with a lentiviral vector to overexpress endogenous miR-126a-5p (Pre-126), a lentiviral vector that inhibits endogenous miR-126a-5p (LAN-126), as well as an empty lentiviral vector, which was used as a control (Pre-Ctrl). The infection efficiency of lentiviral vector was ~75%. The endogenous miR-126a-5p expression in Pre-126- and LAN-126-transfected RPMECs was significantly higher and lower than that of the control group, respectively (Supplementary Figure S3).

Involvement of miR-126a-5p in the PI3K/p-AKT pathway

We aimed at elucidating the molecular mechanisms involved in miR-126a-5p-mediated EndMT. We investigated the expression pattern of the genes belonging to the TGF-β family and found that the TGF-β2 target gene has eight complementary bases with miR-126a-5p (Figure 4c). Furthermore, the ELISA results showed decreased secreted TGF-β2 in cells transfected with Pre-126 and increased levels in cells treated with the miR-126a-5p inhibitor. However, the difference was not statistically significant. When comparing TGF-β2 expression in RPMECs subjected to hypoxia to those from normoxic cells, a decrease in secreted TGF-β2 levels was observed from 24–72 h (Supplementary Figure S4). Therefore, we performed luciferase reporter assays, which confirmed that TGF-β2 was not the direct target gene of miR-126a-5p (Supplementary Figure S4).

The role of PI3K/p-AKT signaling in the miR-126a-5p-mediated EndMT of RPMECs has not been previously elucidated. We first confirmed that the PI3K/p-AKT pathway was involved in miR-126a-5p regulation at the protein expression level. We found that 48 h of hypoxia treatment of RPMECs caused a significant decrease in the expression of Pecam1 and an increase in α-SMA expression. Moreover, transfection with LAN-126 followed by treatment for 48 h with hypoxia led to a significant increase in the level of Pecam1 and a decrease in α-SMA expression (Figures 6a,b). In addition, our results suggested that transfection with LAN-126 followed by 48 h of hypoxia conditions increased the expression of phosphatidylinositol 3 kinase (PI3K) (p85β) and phosphorylation of AKT at the serine 473 site compared with the negative control group. PI3K (p110α) was not significantly altered by miR-126a-5p inhibition and hypoxia treatment (Figures 6c–f). These data showed that knockdown of miR-126a-5p could ameliorate EndMT after 48 h of hypoxia via regulating p85-β/p-AKT protein.

Table 1 Microarray analysis of miRNAs (log2 |fold change| ⩾ 0.585 and $P<0.05$)

Name	*Fold changes log2 (ratio)*	P-*value*
rno-miR-19a-3p	0.6047	0.0266
rno-miR-218a-5p	0.5984	0.0091
rno-miR-3588	0.7749	0.0143
rno-miR-532-5p	0.6482	0.0151
rno-miR-551b-3p	0.6183	0.0192
rno-miR-126a-5p	0.6247	0.0120
rno-let-7b-5p	−0.6090	0.0214
rno-miR-210-3p	−0.7000	0.0079

Abbreviation: miRNA, microRNA.

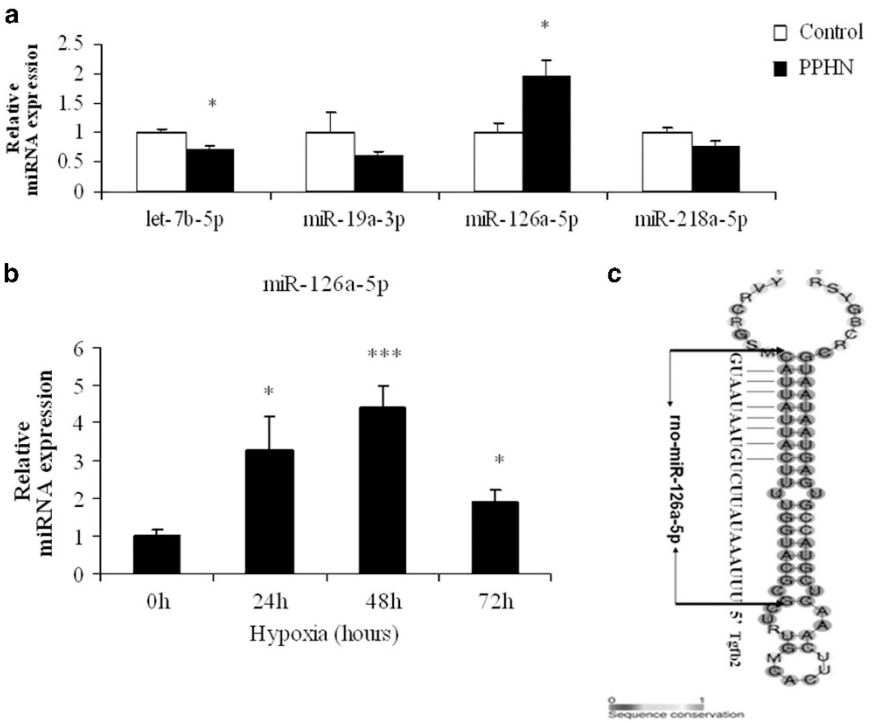

Figure 4 (**a**) Real-time qRT-PCR analysis of the four miRNA levels obtained in the lungs after 14 days of hypoxia ($n=6$ per group). The data are expressed as miRNA/U6 ratios. *$P<0.05$ PPHN *vs.* normoxia. (**b**) Real-time qRT-PCR analysis of the miR-126a-5p levels. The data are expressed as miR-126a-5p/U6 ratios. *$P<0.05$ Hypoxia *vs.* normoxia, ***$P<0.001$ Hypoxia *vs.* normoxia. (**c**) The TGF-β2 target gene has eight complementary bases with miR-126a-5p. PPHN, persistent pulmonary hypertension of the newborn. A full color version of this figure is available at *Hypertension Research* online.

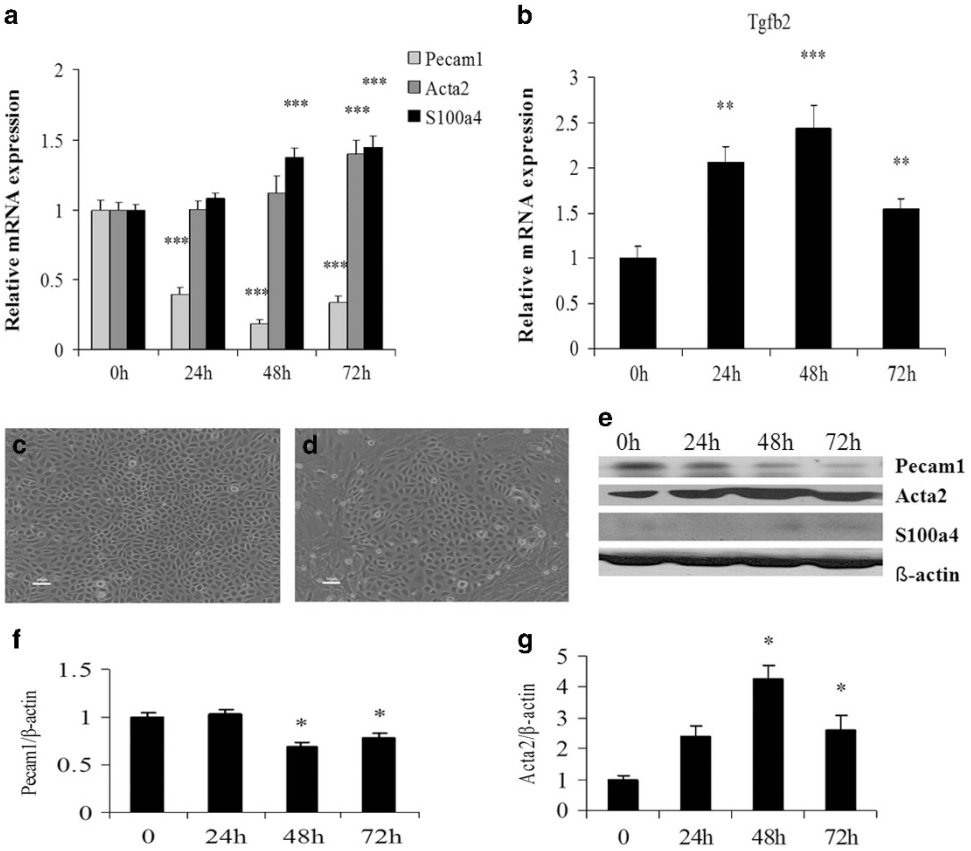

Figure 5 (**a**) Real-time qRT-PCR analysis of the mRNA levels of three genes after hypoxia treatment for 24–72 h. (**b**) Real-time qRT-PCR analysis of the TGF-β2 mRNA levels. The data are expressed as the ratio of the expression of the genes to β-actin. (**c**) RPMECs. (**d**) Hypoxia-treated RPMECs after 48 h. (**e**–**g**) Western blot results from RPMECs. Graphic representations of the ratios of Pecam1 and α-SMA measurements (mean ± s.e.m.) using image analysis. $^{*}P<0.05$ Hypoxia *vs.* normoxia, $^{**}P<0.01$ Hypoxia *vs.* normoxia, $^{***}P<0.001$ Hypoxia *vs.* normoxia ($n=6$ per group). α-SMA, alpha smooth muscle actin; Pecam1, platelet/endothelial cell adhesion molecule-1; RPMEC, rat pulmonary microvascular endothelial cells. A full color version of this figure is available at the *Hypertension Research* journal online.

Comparison of the miR-126a-5p serum levels in PPHN and healthy neonates

The circulating miR-126a-5p concentration was clearly upregulated in PH patients compared with healthy neonates. Of the 18 infants included in this study, 7 had PH as defined in the Materials and methods section. The etiology of PH in the group was meconium aspiration syndrome ($n=2$), meconium aspiration syndrome and perinatal asphyxia ($n=1$), congenital diaphragmatic hernia ($n=1$), respiratory distress syndrome ($n=2$) and sepsis ($n=1$). The patient characteristics of the groups are shown in Table 2. No significant differences were found between the PH and control groups for gestational age, birth weight, gender, mode of delivery and age of presentation. Using real-time PCR, we analyzed the expression of miR-126a-5p in PH patients and in healthy neonates. The results are summarized in Figure 7. The serum miR-126a-5p levels showed significant correlations with oxygenation index ($r=0.890$, $P=0.043$). There was no significant correlation among the serum miR-126a-5p levels, AaDO2 and blood pressure support scoring.

DISCUSSION

Hypoxic pulmonary vasoconstriction is a homeostatic mechanism that is intrinsic to the pulmonary vasculature.[16] Hypoxic pulmonary vasoconstriction is thought to be responsible for restricting blood flow through fetal pulmonary circulation before birth and for matching perfusion to ventilation thereafter, thereby restoring V'_A/Q' equilibrium. The vicious cycle of hypoxemia induces further decreases in pulmonary perfusion and systemic hypoxemia. Under conditions of chronic hypoxemia, generalized pulmonary vascular remodeling may be associated with the EndMT. Here, we present evidence that the EndMT is a central component in the remodeling of the small pulmonary arteries that occurs during hypoxia-induced PPHN. The EndMT is a complex biological process characterized by the loss of endothelial-specific markers, such as Pecam1 (also known as CD31), and the gain of mesenchymal markers such as S100a4 (also known as fibroblast-specific protein 1, FSP1) and α-SMA.[17] EndMT is stimulated by some environmental cues. It is essential for processes involved in embryonic development and can be pathologically dysregulated in disease states.[18] Mihira *et al.*[19] demonstrated evidence of endothelial cell plasticity, which allows these cells to undergo the EndMT *in vitro*. TGF-β2 plays pivotal roles in both the epithelial–mesenchymal transition and the EndMT, and it is involved in multiple downstream mechanisms, depending on the cell context.[19,20] Interestingly, pulmonary endothelial cells also play a role in pathological conditions, for instance, by differentiating into mesenchymal cells, increasing α-SMA and S100a4 expression, and by participating in intimal thickening and pulmonary vascular remodeling. *In vivo*, the small pulmonary arteries in the PPHN group demonstrated an increased level of α-SMA, and *in vitro,* primary neonatal RPMECs underwent EndMT after exposure to hypoxia. In our study, the protein expression of Pecam1 by immunohistochemistry revealed no significant decrease

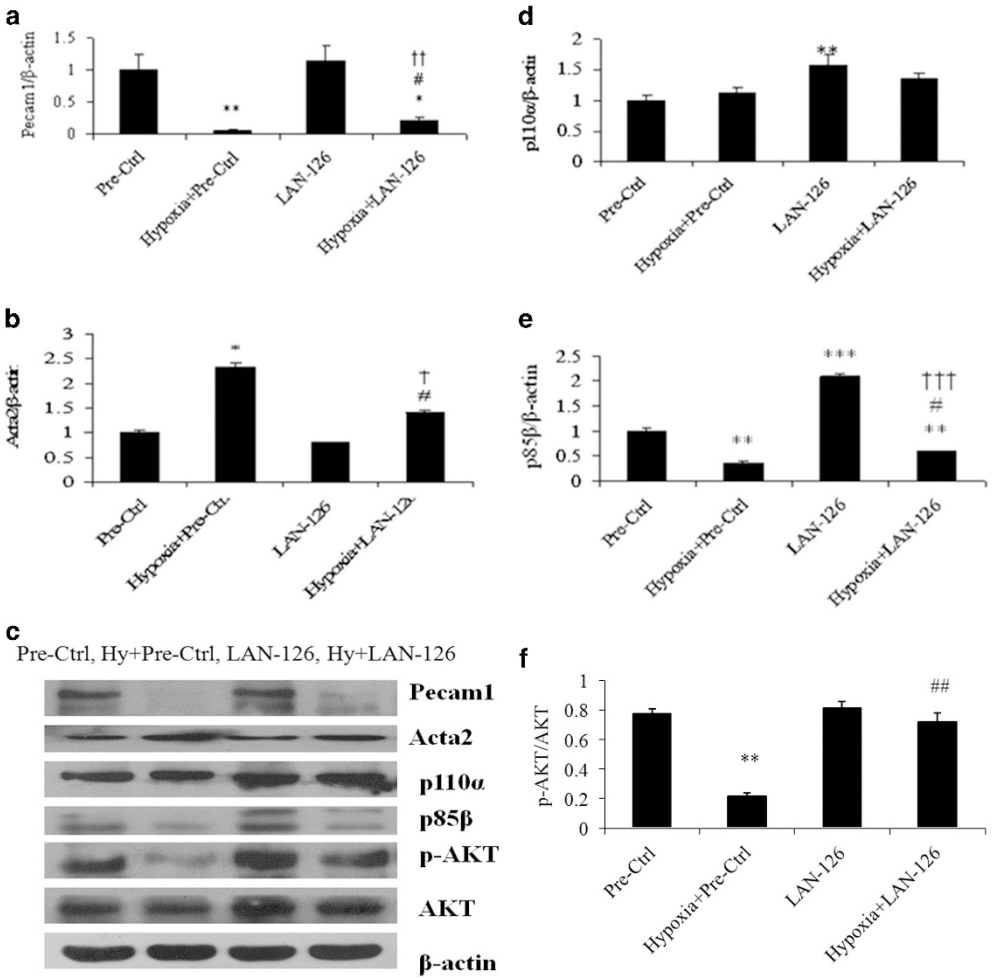

Figure 6 Western blot results from RPMECs transfected with LAN-126 and then exposed to 48 h of hypoxia (**c**). (**a**,**b**,**d**,**e**,**f**) Graphic representations of the ratio of the protein measurements (mean ± s.e.m.) using image analysis, $^{*}P<0.05$, $^{**}P<0.01$ Hypoxia *vs.* Pre-Ctrl, $^{\dagger}P<0.05$, $^{\dagger\dagger}P<0.01$ Hypoxia+LAN-126 *vs.* LAN-126; $^{\#}P<0.05$, $^{\#\#}P<0.01$ Hypoxia+LAN-126 *vs.* Hypoxia+Pre-Ctrl, ($n=6$ per group). RPMEC, rat pulmonary microvascular endothelial cells.

Table 2 Clinical characteristics of PPHN and healthy infants

	PPHN (n = *7*)	*Control* (n = *11*)	P-*value*
Gestational age, week, mean (s.e.)	37.3 ± 1.4	37.1 ± 1.1	0.912
Birth weight, g, mean (s.e.)	2944.3 ± 395.5	2909.1 ± 195.6	0.930
Male	3	7	0.263
1-minute Apgar score, median	10 (5,10)	10 (10,10)	0.146
5-minute Apgar score, median	10 (8,10)	10 (10,10)	0.339
Mode of delivery	4/7	3/11	0.205
Age of presentation (within 3 days after birth)	4	8	0.494

Abbreviation: PPHN, persistent pulmonary hypertension of the newborn.

in vivo and a significant decrease for the mRNA expression of Pecam1 *in vitro*. It is well known that *in vitro*, the influencing factors are single and controllable, and *in vivo,* observations are complex because the organism maintains a stable internal environment using specific proteins. Immunohistochemistry is a semi-quantitative assessment because of unspecific background labeling. Thus, we did further western blot quantitative analysis of Pecam1 protein *in vitro*. Recent research showed that western blot analysis and immunofluorescence demonstrated decreased expression levels of Pecam1 proteins at both 12-h and 24-h hypoxia exposure time points,[21] which is consistent with the results of our study. These results raise the question of how the EndMT process of primary neonatal RPMECs is regulated.

One of the main aims of this study was to establish the molecular mechanisms driving the EndMT process. Previous research has shown that the levels of specific miRNAs known to be dysregulated in different cardiovascular diseases are altered during EndMT.[22] The epigenetic regulators of gene expression at the posttranscriptional level are involved in the EndMT and promote profibrotic signaling in EndMT-derived fibroblast-like cells. To our knowledge, no study has investigated the miRNA profiles during the vascular remodeling associated with PPHN. We used miRNA arrays to analyze lung tissues from a hypoxia-induced PPHN rat model and identified a pool of differentially expressed miRNAs. We validated four of the most interesting candidate miRNAs. We focused on miR-126a-5p, an endothelial-specific miRNA enriched in endothelial cells that regulates endothelial cell proliferation, mobilization and migration.[23,24] Targeted deletion of miR-126 causes the loss of vascular integrity in mice and zebrafish during development, resulting in defective angiogenesis.[25,26] Our study suggests that miR-126a-5p is involved in the EndMT process. With miR-126a-5p inhibition, the mRNA

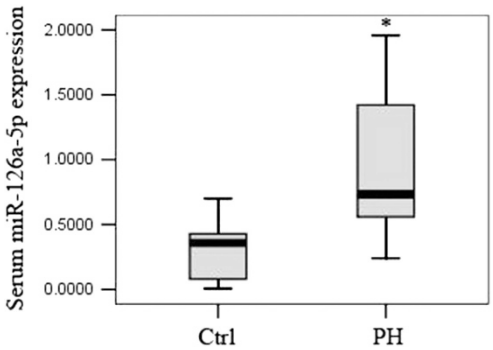

Figure 7 Real-time PCR showing the expression of miR-126a-5p in PH patients and in healthy neonates. $*P<0.05$ PH *vs.* Ctrl. PH, pulmonary hypertension. A full color version of this figure is available at *Hypertension Research* online.

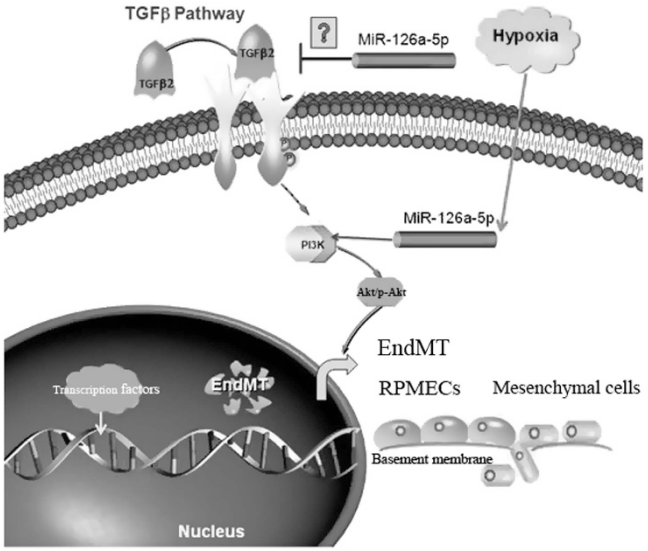

Figure 8 The scheme of the hypoxia/miR-126a-5p/PI3K (p85-ß)/p-Akt/EndMT and TGF-β2 pathway. A full color version of this figure is available at *Hypertension Research* online.

expression of the endothelial-specific marker Pecam1 was upregulated in RPMECs. The overexpression of miR-126a-5p in RPMECs increased the protein levels of the mesenchymal cell marker S100a4. However, screening for the potential targets of miR-126a-5p is a challenging process because prediction algorithms generate a high proportion of false positives. TGF-β2 is a predicted potential target of miR-126a-5p in the miRNA database, and several studies have demonstrated the important roles of TGF-β2 signaling and its downstream targets in EndMT.[27–31] The ablation of TGF-β2 in mice prevents EndMT-mediated cardiac development. However, TGF-β1 or TGF-β3 knockout mice showed no significant defects in EndMT or heart development.[32] The results of the present study provide novel insight into the signaling mechanisms that mediate the EndMT. We have shown that miR-126a-5p expression is increased and that TGF-β2 mRNA expression is upregulated. TGF-β2 protein secretion decreased during hypoxia, which may be the self-limiting dynamics of TGF-β2, which are regulated by negative feedback. However, the application of TGF-β2 (3 ng ml^{-1}) for 7 days did not alter miR-126a-5p expression (data not shown), and a luciferase reporter assay showed that TGF-β2 is not a direct target of miR-126a-5p. Our next study may focus on the downstream pathway of TGF-β2. On the basis of these findings, we concluded that TGF-β2 is not a direct target of the miR-126a-5p-mediated EndMT process in RPMECs.

PI3K is a lipid kinase that phosphorylates phosphatidylinositol and similar compounds, creating second messengers that are important in growth signaling pathways. It contains a p110 catalytic subunit and a p85 regulatory subunit. The protein p85 also suppresses activation of the PI3K/AKT signaling pathway.[33] Currently, the elucidation of signaling pathways has led to new advances in the understanding of the mechanisms of PPHN, including the PI3K-protein kinase B (Akt) pathway. As previously described, miR-126 inhibits the expression of the PI3K/Akt signaling pathway, indicating that miR-126 could regulate the target gene and inhibit the PI3K/Akt signaling pathway.[34] miR-126 has been previously shown to act through the PI3K/AKT and MAPK/ERK pathways, and the increased release of paracrine factors partly promotes the differentiation toward endothelial cells.[35,36] Chen and Zhou[37] reported that miR-126 induced the phosphorylation of AKT in mesenchymal stem cells without exogenous stimulation. Endothelial-specific miR-126-5p was excised from EGFL7 pre-mRNA without affecting the splicing and expression of its host gene, so miR-126a-5p expression is likely to be mediated via PI3K/Akt signaling through a negative feedback loop.[38] In this study, interestingly, our findings showed that miR-126a-5p is specifically involved in the PI3K/p-AKT pathway in the EndMT process in RPMECs. The levels of p85 and p-AKT decreased in hypoxia-treated RPMECs after 48 h, and this was concurrent with miR-126a-5p overexpression. These results are consistent with the previous findings in CRL-1730 cells that the overexpression of miR-126 reduced p85-β expression.[39] Thus, the PI3K/p-AKT pathway is likely an important mediator of the effects of the EndMT process in RPMECs by regulating miR-126a-5p expression. Our study also showed that transfection with miR-126a-5p-inhibiting oligonucleotides ameliorated the reduction in Pecam1 and the increase in α-SMA expression when RPMECs were exposed to hypoxia. P85-β/p-AKT signaling was activated in cells transfected with a miR-126a-5p inhibitor compared with the Hypoxia+Pre-Ctrl group. Taken together, these findings imply that the knockdown of miR-126a-5p inhibited the RPMEC EndMT by involving p85-β/p-AKT signaling.

After verifying the role of miR-126a-5p in a rat model of PPHN and in hypoxia-induced RPMECs, we assessed its possible use as a novel and promising biomarker in body fluids because circulating miRNAs are stable in serum.[40] In this study, we demonstrated that serum miR-126a-5p levels were increased in PPHN patients compared with those in healthy controls and that the levels correlated with disease severity. However, this part of the study was limited by the small sample size, and more subjects are required in future studies. We hope to perform *in vivo* experiments with gain/loss of function of miR-126a-5p and see the effects on the structural remodeling of the pulmonary vasculature in the PPHN model in the future.

In summary, the data presented in this study suggest that the upregulation of miR-126a-5p in PPHN may contribute to the hypoxia-induced EndMT in RPMECs. We also found that inhibition of miR-126a-5p ameliorates the EndMT process and that the mechanism underlying hypoxia-induced miR-126a-5p upregulation probably acts through the p85-β/p-AKT pathway, but not by directly targeting TGF-β2 expression (Figure 8).

CONFLICT OF INTEREST

The authors declare no conflict of interest.

ACKNOWLEDGEMENTS

This work was supported by the Central Laboratory of the Children's Hospital of Zhejiang University School of Medicine and the Zhejiang Key Laboratory for Diagnosis and Therapy of Neonatal Diseases. We thank Dr Henry Akinbi (Cincinnati Children's Hospital Medical Center, Cincinnati, Ohio) for carefully reviewing the manuscript. This work was supported by grants from the National Natural Science Foundation of China (No. 81200460, 81471480 and 81630037).

1 Walsh-Sukys MC, Tyson JE, Wright LL, Bauer CR, Korones SB, Stevenson DK, Verter J, Stoll BJ, Lemons JA, Papile LA, Shankaran S, Donovan EF, Oh W, Ehrenkranz RA, Fanaroff AA. Persistent pulmonary hypertension of the newborn in the era before nitric oxide: practice variation and outcomes. *Pediatrics* 2000; **105**: 14–20.
2 Stenmark KR, Abman SH. Lung vascular development: implications for the pathogenesis of bronchopulmonary dysplasia. *Annu Rev Physiol* 2005; **67**: 623–661.
3 Stenmark KR, Fagan KA, Frid MG. Hypoxia-induced pulmonary vascular remodeling: cellular and molecular mechanisms. *Circ Res* 2006; **99**: 675–691.
4 Stenmark KR, Meyrick B, Galie N, Mooi WJ, McMurtry IF. Animal models of pulmonary arterial hypertension: the hope for etiological discovery and pharmacological cure. *Am J Physiol Lung Cell Mol Physiol* 2009; **297**: L1013–L1032.
5 Vosatka RJ. Persistent pulmonary hypertension of the newborn. *N Engl J Med* 2002; **346**: 864.
6 Yun X, Chen Y, Yang K, Wang S, Lu W, Wang J. Upregulation of canonical transient receptor potential channel in the pulmonary arterial smooth muscle of a chronic thromboembolic pulmonary hypertension rat model. *Hypertens Res* 2015; **38**: 821–828.
7 Haworth SG, Hislop AA. Lung development-the effects of chronic hypoxia. *Semin Neonatol* 2003; **8**: 1–8.
8 Young KC, Torres E, Hatzistergos KE, Hehre D, Suguihara C, Hare JM. Inhibition of the SDF-1/CXCR4 axis attenuates neonatal hypoxia-induced pulmonary hypertension. *Circ Res* 2009; **104**: 1293–1301.
9 Cooley BC, Nevado J, Mellad J, Yang D, St HC, Negro A, Fang F, Chen G, San H, Walts AD, Schwartzbeck RL, Taylor B, Lanzer JD, Wragg A, Elagha A, Beltran LE, Berry C, Feil R, Virmani R, Ladich E, Kovacic JC, Boehm M. TGF-β signaling mediates endothelial-to-mesenchymal transition (EndMT) during vein graft remodeling. *Sci Transl Med* 2014; **6**: 227ra34.
10 Sessa R, Hata A. Role of microRNAs in lung development and pulmonary diseases. *Pulm Circ* 2013; **3**: 315–328.
11 Caruso P, MacLean MR, Khanin R, McClure J, Soon E, Southgate M, MacDonald RA, Greig JA, Robertson KE, Masson R, Denby L, Dempsie Y, Long L, Morrell NW, Baker AH. Dynamic changes in lung microRNA profiles during the development of pulmonary hypertension due to chronic hypoxia and monocrotaline. *Arterioscler Thromb Vasc Biol* 2010; **30**: 716–723.
12 Xu YP, Zhu JJ, Cheng F, Jiang KW, Gu WZ, Shen Z, Wu YD, Liang L, Du LZ. Ghrelin ameliorates hypoxia-induced pulmonary hypertension via phospho-GSK3 β/β-catenin signaling in neonatal rats. *J Mol Endocrinol* 2011; **47**: 33–43.
13 John TA, Ibe BO, Usha RJ. Oxygen alters caveolin-1 and nitric oxide synthase-3 functions in ovine fetal and neonatal lung microvascular endothelial cells. *Am J Physiol Lung Cell Mol Physiol* 2006; **291**: L1079–L1093.
14 Vijlbrief DC, Benders MJ, Kemperman H, van Bel F, de Vries WB. B-type natriuretic peptide and rebound during treatment for persistent pulmonary hypertension. *J Pediatr* 2012; **160**: 111–115.e1.
15 Krediet TG, Valk L, Hempenius I, Egberts J, van Bel F. Nitric oxide production and plasma cyclic guanosine monophosphate in premature infants with respiratory distress syndrome. *Biol Neonate* 2002; **82**: 150–154.
16 Dunham-Snary KJ, Wu D, Sykes EA, Thakrar A, Parlow LR, Mewburn JD, Parlow JL, Archer SL. Hypoxic pulmonary vasoconstriction: from molecular mechanisms to medicine. *Chest* 2016; **151**: 181–192.
17 Lin F, Wang N, Zhang TC. The role of endothelial-mesenchymal transition in development and pathological process. *IUBMB Life* 2012; **64**: 717–723.
18 Schindeler A, Kolind M, Little DG. Cellular transitions and tissue engineering. *Cell Reprogram* 2013; **15**: 101–106.
19 Mihira H, Suzuki HI, Akatsu Y, Yoshimatsu Y, Igarashi T, Miyazono K, Watabe T. TGF-β-induced mesenchymal transition of MS-1 endothelial cells requires Smad-dependent cooperative activation of Rho signals and MRTF-A. *J Biochem* 2012; **151**: 145–156.
20 Saito A. EMT and EndMT: regulated in similar ways. *J Biochem* 2013; **153**: 493–495.
21 Souvannakitti D, Peerapen P, Thongboonkerd V. Hypobaric hypoxia down-regulated junctional protein complex: implications to vascular leakage. *Cell Adh Migr* (e-pub ahead of print 14 September 2016; doi:10.1080/19336918.2016.1225633).
22 Ghosh AK, Nagpal V, Covington JW, Michaels MA, Vaughan DE. Molecular basis of cardiac endothelial-to-mesenchymal transition (EndMT): differential expression of microRNAs during EndMT. *Cell Signal* 2012; **24**: 1031–1036.
23 Potus F, Graydon C, Provencher S, Bonnet S. Vascular remodeling process in pulmonary arterial hypertension, with focus on miR-204 and miR-126 (2013 Grover Conference series). *Pulm Circ* 2014; **4**: 175–184.
24 Liebner S, Cattelino A, Gallini R, Rudini N, Iurlaro M, Piccolo S, Dejana E. Beta-catenin is required for endothelial-mesenchymal transformation during heart cushion development in the mouse. *J Cell Biol* 2004; **166**: 359–367.
25 Zou J, Li WQ, Li Q, Li XQ, Zhang JT, Liu GQ, Chen J, Qiu XX, Tian FJ, Wang ZZ, Zhu N, Qin YW, Shen B, Liu TX, Jing Q. Two functional microRNA-126s repress a novel target gene p21-activated kinase 1 to regulate vascular integrity in zebrafish. *Circ Res* 2011; **108**: 201–209.
26 Fish JE, Santoro MM, Morton SU, Yu S, Yeh RF, Wythe JD, Ivey KN, Bruneau BG, Stainier DY, Srivastava D. miR-126 regulates angiogenic signaling and vascular integrity. *Dev Cell* 2008; **15**: 272–284.
27 Medici D, Potenta S, Kalluri R. Transforming growth factor-β2 promotes Snail-mediated endothelial-mesenchymal transition through convergence of Smad-dependent and Smad-independent signalling. *Biochem J* 2011; **437**: 515–520.
28 Kokudo T, Suzuki Y, Yoshimatsu Y, Yamazaki T, Watabe T, Miyazono K. Snail is required for TGFbeta-induced endothelial-mesenchymal transition of embryonic stem cell-derived endothelial cells. *J Cell Sci* 2008; **121**: 3317–3324.
29 Deissler H, Deissler H, Lang GK, Lang GE. TGFbeta induces transdifferentiation of iBREC to alphaSMA-expressing cells. *Int J Mol Med* 2006; **18**: 577–582.
30 Tavares AL, Mercado-Pimentel ME, Runyan RB, Kitten GT. TGF beta-mediated RhoA expression is necessary for epithelial-mesenchymal transition in the embryonic chick heart. *Dev Dyn* 2006; **235**: 1589–1598.
31 Zeng L, Wang G, Ummarino D, Margariti A, Xu Q, Xiao Q, Wang W, Zhang Z, Yin X, Mayr M, Cockerill G, Li JY, Chien S, Hu Y, Xu Q. Histone deacetylase 3 unconventional splicing mediates endothelial-to-mesenchymal transition through transforming growth factor β2. *J Biol Chem* 2013; **288**: 31853–31866.
32 Azhar M, Runyan RB, Gard C, Sanford LP, Miller ML, Andringa A, Pawlowski S, Rajan S, Doetschman T. Ligand-specific function of transforming growth factor beta in epithelial-mesenchymal transition in heart development. *Dev Dyn* 2009; **238**: 431–442.
33 Ueki K, Fruman DA, Yballe CM, Fasshauer M, Klein J, Asano T, Cantley LC, Kahn CR. Positive and negative roles of p85 alpha and p85 beta regulatory subunits of phosphoinositide 3-kinase in insulin signaling. *J Biol Chem* 2003; **278**: 48453–48466.
34 Xiao J, Lin HY, Zhu YY, Zhu YP, Chen LW. MiR-126 regulates proliferation and invasion in the bladder cancer BLS cell line by targeting the PIK3R2-mediated PI3K/Akt signaling pathway. *Onco Targets Ther* 2016; **9**: 5181–5193.
35 Huang F, Fang ZF, Hu XQ, Tang L, Zhou SH, Huang JP. Overexpression of miR-126 promotes the differentiation of mesenchymal stem cells toward endothelial cells via activation of PI3K/Akt and MAPK/ERK pathways and release of paracrine factors. *Biol Chem* 2013; **394**: 1223–1233.
36 Zhang J, Zhang Z, Zhang DY, Zhu J, Zhang T, Wang C. microRNA 126 inhibits the transition of endothelial progenitor cells to mesenchymal cells via the PIK3R2-PI3K/Akt signalling pathway. *PLoS ONE* 2013; **8**: e83294.
37 Chen JJ, Zhou SH. Mesenchymal stem cells overexpressing MiR-126 enhance ischemic angiogenesis via the AKT/ERK-related pathway. *Cardiol J* 2011; **18**: 675–681.
38 Li Y, Zhou Q, Pei C, Liu B, Li M, Fang L, Sun Y, Li Y, Meng S. Hyperglycemia and advanced glycation end products regulate miR-126 expression in endothelial progenitor cells. *J Vasc Res* 2016; **53**: 94–104.
39 Sui XQ, Xu ZM, Xie MB, Pei DA. Resveratrol inhibits hydrogen peroxide-induced apoptosis in endothelial cells via the activation of PI3K/Akt by miR-126. *J Atheroscler Thromb* 2014; **21**: 108–118.
40 Turchinovich A, Weiz L, Langheinz A, Burwinkel B. Characterization of extracellular circulating microRNA. *Nucleic Acids Res* 2011; **39**: 7223–7233.

Supplementary Information accompanies the paper on Hypertension Research website (http://www.nature.com/hr)